

# Observation of Nanosecond Carrier Pulses

KAZUHIRO MIYAUCHI

**Summary**—The present paper describes theory and experiments on the observation of nanosecond carrier pulses in the microwave region. The advancement of microwave nanosecond techniques requires measurement of waveforms which is more accurate than conventional methods. The measuring method described here was developed to satisfy this requirement. The new method, using a synchronous or heterodyne detector, gives accurate and complete information on nanosecond pulse waveforms in the microwave region. Applying this method, we constructed an experimental system to generate and observe the nanosecond pulses in the 11-Gc region. The over-all rise and fall time and delay resolution of this system are as small as 0.5 nsec. Pulse modulators, detectors and filters were measured or adjusted with this experimental system. The experimental results are described in this paper. The pulse generation and observation system developed here is expected to be useful for measuring and adjusting microwave nanosecond pulse devices with accuracy.

## INTRODUCTION

**I**N RECENT YEARS nanosecond pulse techniques in the microwave and millimeter wave region have attracted much attention. Many investigations have been made on high-speed pulse communications, high-speed electronic computers and circuit measurements.

Usual microwave nanosecond pulse techniques have some weak points in the waveform observation, because they employ quadratic detectors which afford waveform information on the power waveform base. The advancement of techniques requires more accurate measurements on the amplitude base in order to test and adjust the response of microwave pulse devices.

The author performed experiments on a traveling-wave tube pulse generator at the 24-Gc.<sup>1</sup> It was found that the observation of waveforms is particularly important. It is believed that precise experiments on the processing of microwave pulses could not be made without measuring the waveforms accurately.

The observation of microwave nanosecond pulses on the amplitude base has been tried. A. F. Dietrich<sup>2</sup> observed instantaneous amplitude waveforms of 8- and 11-Gc carrier pulses by means of a new technique which may be called a "Microwave Sampling Oscilloscope." But his technique can be applied only to a pulse train whose carrier phase is locked to the envelope. Ordinary nanosecond pulse trains in the microwave region do not have the carrier phase locked to the envelope because they are obtained by the switching of continuous carrier.

Manuscript received March 11, 1963; revised December 9, 1963.

The author is with the Nippon Telephone and Telegraph Public Corporation, Musashino-shi, Tokyo, Japan.

<sup>1</sup> K. Miyuchi, "Traveling-wave tube nanosecond pulse generator in 24-Gc region," *IEEE TRANS. ON MICROWAVE THEORY AND TECHNIQUES*, vol. MTT-11, pp. 3-17; January, 1963.

<sup>2</sup> A. F. Dietrich, "8- and 11-Gc nanosecond carrier pulses produced by harmonic generation," *PROC. IRE*, vol. 49, pp. 972-973; May, 1961.

It is thought that this method cannot be applied directly to these types of pulse trains.

W. M. Goodall and A. F. Dietrich<sup>3</sup> developed a type of sampling oscilloscope whose pass band extends to the microwave region. Employing this oscilloscope, the instantaneous amplitude waveforms of microwave nanosecond pulses can be observed when the carrier frequency is smaller than several gigacycles, but their method cannot be applied to pulses having carrier frequencies larger than that.

The author's preceding method differs from the techniques which are based on the observation of instantaneous amplitude waveforms. He employs a synchronous or heterodyne detector to obtain the in-phase and quadratic components or the envelope of microwave nanosecond pulses.

## DESCRIPTION OF MEASUREMENT PRINCIPLES

It is well known that the characteristics of an RF pulse are described with two time functions. The following two expressions are ordinarily used:

$$G(t) = g(t) \cos [\omega_0 t + \phi(t)] \quad (1)$$

$$G(t) = I(t) \cos (\omega_0 t + \theta_0) - Q(t) \sin (\omega_0 t + \theta_0), \quad (2)$$

where

$G(t)$  = instantaneous amplitude of RF pulse

$t$  = time

$g(t)$  = envelope

$\omega_0$  = angular frequency of carrier

$\phi(t)$  = carrier phase modulation

$I(t)$  = in-phase component

$Q(t)$  = quadrature component

$\theta_0$  = constant phase.

One expression employs  $g(t)$  and  $\phi(t)$ , and the other,  $I(t)$  and  $Q(t)$ . Those two expressions are equivalent. The following relations hold:

$$I(t) = g(t) \cos [\phi(t) - \theta_0], \quad Q(t) = g(t) \sin [\phi(t) - \theta_0] \quad (3)$$

$$g^2(t) = I^2(t) + Q^2(t), \quad \tan [\phi(t) - \theta_0] = Q(t)/I(t). \quad (4)$$

The pulse observation system now in general use is composed of a quadratic detector and a sampling oscilloscope. It has many disadvantages, such as

- 1) Lack of phase information. The quadratic detector gives  $g(t)$  only. The carrier phase modulation  $\phi(t)$  cannot be observed.

<sup>3</sup> W. M. Goodall and A. F. Dietrich, "Fractional millimicrosecond electrical stroboscope," *PROC. IRE*, vol. 48, pp. 1591-1595; September, 1960.

TABLE I  
MAIN CHARACTERISTICS OF SYNCHRONOUS AND HETERODYNE DETECTION

	Synchronous Detection	Heterodyne Detection	
		Phase Lock Type	Phase Random Type
Information	complete	complete	incomplete
Sensitivity	good*	good*	good*
Linearity	good	good	good
Observation of Envelope	indirect	direct	direct
Observation of Residual Carrier	indirect	direct	direct
Observation of Instantaneous Phase	indirect but accurate	direct but inaccurate	not
Observation of In-phase and Quadrature Components	direct	indirect	not
Applicability of Concepts based on Linear Mathematical Operations	completely available	completely available	available but incomplete
Dynamic Range	wide†	wide†	wide†
Operation of Phase Control	necessary	unnecessary	unnecessary

\* It is observed experimentally<sup>4</sup> and theoretically<sup>5</sup> that the sensitivity of those detection systems are better than that of the quadratic detection system more than 20 db in the case when they are used together with a sampling oscilloscope of commercial quality.

† About 40 db or more.

- 2) Poor sensitivity.
- 3) Poor linearity. Diode characteristics deviate from the strictly quadratic ones in many cases.
- 4) Many problems arise from the fact that the observation is based on power waveforms and not on amplitude waveforms. We cannot use directly the following concepts which are based on the linear mathematical operations and useful for analyzing the experimental results in the case of baseband pulse techniques: a) superposition of instantaneous amplitude, b) half amplitude duration, c) amplitude rise and fall times, d) overshoot and undershoot, e) sag, f) relation between rise time and bandwidth, and g) over-all rise time of circuits connected in cascade.
- 5) Narrow dynamic range. A wide dynamic range is required for accurate observation of waveforms, especially for observing the leading and trailing edges of a pulse and weak echoes.

The author employed synchronous and heterodyne detectors for the observation. The detector output is connected to a sampling oscilloscope. The synchronous detector is especially useful for precise measurements. The above disadvantages of quadratic detection are all lessened by using the detector.

The author studied the characteristics of those detectors when they are used together with a sampling oscilloscope.<sup>4,5</sup> Table I briefly shows results of the study.

<sup>4</sup> K. Miyauchi, "Nanosecond Pulse Generation using Semiconductor Diode in 24-Gc Region," *Proc. Conf. No. 948, Inst. Elec. Commun. Engrs. of Japan*, Tokyo, Japan; April, 1962.

<sup>5</sup> K. Miyauchi, "Microwave Pulse Measurements by Means of Sampling Oscilloscope Principles," unpublished report.

Fig. 1 is a block diagram of the pulse generation and observation system employing a synchronous detector. When a circuit or a transmission line is tested by this system, it is inserted between the pulse modulator and the detector.

Sensitivity of this observation system is determined by the conversion loss of the detector and the sampling circuit noise of the oscilloscope. The noise output of the detector diode has little contribution to the over-all noise presentation on the oscilloscope because the noise of sampling diode is large when a sampling oscilloscope of commercial quality is used.

The conversion loss of the synchronous or heterodyne detector is superior to that of the quadratic detector by 20 db or more for microwave input power as small as 1 microwatt. Therefore, the sensitivity of the observation system is improved by 20 db or more if the synchronous or heterodyne detector is used.<sup>6</sup>

The linearity of the synchronous or heterodyne detector is inherently good when the signal power is much smaller than the local power. The dynamic range of the observation is equal to that of the oscilloscope when the synchronous or heterodyne detector is used. Therefore, it is about 40 db. On the other hand, the quadratic detector gives a dynamic range of about 20 db because it is half value of the oscilloscope dynamic range in db.

Let the signal waveform incident to the synchronous detector be (1), and the local waveform be

$$E(t) = E_L \cos(\omega_L t + \theta). \quad (5)$$

<sup>6</sup> If the noise presentation on the sampling oscilloscope is much reduced, more improvement will be obtained.

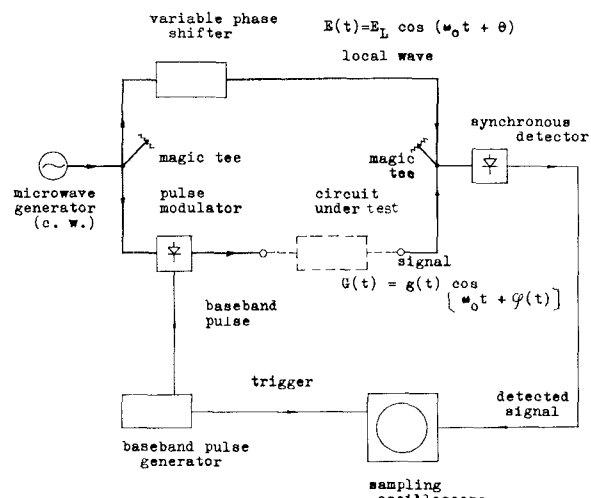


Fig. 1—Pulse generation and observation system employing a synchronous detector (being used to measure the pulse response of circuit under test).

Then the output of the detector is<sup>5</sup>

$$S(t) = H(E_L)g(t) \cos [\phi(t) - \theta], \quad (6)$$

where  $H(E_L)$  is a function of  $E_L$  determined by the nonlinear characteristics of the detector. The phase angle  $\theta$  can be set at a desired value by controlling the variable phase shifter in Fig. 1. Thus we obtain<sup>7</sup>

$$S(t) = H(E_L)g(t) \cos [\phi(t) - \theta_0] = H(E_L)I(t); \quad \theta = \theta_0 \quad (7)$$

$$S(t) = H(E_L)g(t) \sin [\phi(t) - \theta_0] = H(E_L)Q(t); \quad \theta = \theta_0 + (\pi/2). \quad (8)$$

These are proportional to the in-phase and quadrature components of the incident signal waveform. Therefore, complete information on the signal waveform is obtained.

In practical cases, only the relative values of phase angle  $\theta$  and  $\theta_0$  are known. It will be convenient to decide that the in-phase component  $I(t)$  is obtained for the  $\theta$  which makes the peak of observed waveform maximum. Experimental results in this paper are illustrated in accordance with this convenience.

When we employ a heterodyne detector in place of the synchronous detector, the circuit construction becomes as illustrated in Fig. 2.

If a train of signal pulses of (1) is observed by using this circuit, the oscilloscope presents the following waveform (see Appendix I):

$$U(t) = H(E_L)g(t) \cos [\omega_it + \phi(t)], \quad (9)$$

<sup>7</sup> These results are concerned only with the ideal synchronous detector and the ideal oscilloscope. The case employing nonideal devices is treated in Appendix II.

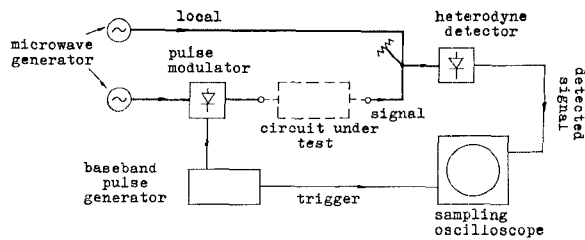


Fig. 2—Example of pulse generation and observation system employing a heterodyne detector.

where

$$\omega_i = - \frac{(MT + \Delta T)\Delta\omega}{\Delta T} - \frac{2\pi}{\Delta T} \left[ \left[ - \frac{(MT + \Delta T)\Delta\omega}{2\pi} \right] \right] \quad (10)$$

$g(t)$  = envelope of original microwave pulse

$\phi(t)$  = carrier phase modulation of original microwave pulse

$\Delta\omega = \omega_1 - \omega_0$  = difference angular frequency

$T$  = period of signal pulse train

$MT + \Delta T$  = period of sampling operation

$M$  = integer

and the symbol  $\left[ [\alpha] \right]$  denotes the largest integer which does not exceed  $\alpha$ .

We will call  $\omega_i$  the "seeming intermediate angular frequency." It is possible to make the seeming intermediate frequency equal to the carrier frequency of original pulses. The condition is

$$\omega_i = \omega_0. \quad (11)$$

It is interesting that (11) is satisfied for very small  $\Delta\omega$ . For example, when  $\Delta\omega$  is so small that the following equation,

$$\left[ \left[ - \frac{(MT + \Delta T)\Delta\omega}{2\pi} \right] \right] = 0, \quad (12)$$

is valid, we obtain

$$\frac{\Delta\omega}{\omega_0} = \frac{-\Delta T}{MT + \Delta T}. \quad (13)$$

For the ordinary sampling oscilloscope,  $\Delta T$  is much smaller than  $MT + \Delta T$ . Therefore,  $\Delta\omega/\omega_0$  is very small.

The above discussion is concerned only with the single sweep operation of the oscilloscope. But, practically, the recurrent sweep is used in the most cases.

In the recurrent sweep, the sweep period should be a multiple of the period of original pulse train. Therefore, we will assume the sweep period is  $kT$  where  $k$  is an integer.

When  $\Delta\omega kT$  is a multiple of  $2\pi$ , the observed waveforms have a fixed RF phase with respect to the envelope. This case will be called the phase lock type in this paper.

When  $\Delta\omega kT$  is not a multiple of  $2\pi$ , the observed waveforms have a successive RF phase precession to the envelope. If this precession uniformly overlaps the area between the positive and negative envelopes, the phase information vanishes on the oscilloscope presentation. This case will be called the phase random type in this paper. The phase lock type is a delicate device to construct. It needs a complete synchronization between the RF carrier phase and the pulse period.

Without the synchronization, the system of Fig. 2 becomes a phase random type. In most cases phase fluctuations of the microwave generators give a substantial random phase of the carrier in the output signal of the heterodyne detector.

The heterodyne detector is useful to measure the constant carrier, the leading and trailing edges of a pulse and weak echoes even when the carrier phase of the pulse to be measured is unknown.

#### PRACTICAL PROCEDURES OF FILTER ADJUSTMENT

The following discussion is concerned with the test or adjustment of a linear microwave circuit, such as a waveguide filter, by use of synchronous detection. In Fig. 1 we will assume that the synchronous detector and the sampling oscilloscope are ideal devices; *i.e.*, the synchronous detector has characteristics independent of frequency in its RF and baseband portions and the sampling oscilloscope has a negligibly small rise time.

In practical cases such devices have nonideal characteristics. But such nonideal cases can be easily reduced to the ideal case as shown in Appendix II. Therefore, the present discussion has complete generality.

At first we will give a rather formal and general treatment. The pulse waveform incident to the synchronous detector is observed in the forms of the in-phase component  $I(t)$  and the quadrature component  $Q(t)$ . From these components we can reconstruct the original pulse waveform as

$$\hat{G}(t) = [I(t) + jQ(t)]e^{j(\omega_0 t + \theta_0)}. \quad (14)$$

We used the vector representation here for convenience. The real part of  $\hat{G}(t)$  is equal to  $G(t)$  defined in the preceding section. The constant phase  $\theta_0$  is introduced in (14) to represent the arbitrariness of phase setting in Fig. 1. By the Fourier transform we obtain the frequency spectrum  $\Omega(f)$  of the pulse waveform  $\hat{G}(t)$

$$\begin{aligned} \Omega(f) &= \int_{-\infty}^{\infty} \hat{G}(t) e^{-j2\pi f t} dt \\ &= e^{j\theta_0} \int_{-\infty}^{\infty} [I(t) + jQ(t)] e^{j2\pi(f-f_0)t} dt. \end{aligned} \quad (15)$$

This means that we can determine  $\Omega(f)$  except for the arbitrary phase  $\theta_0$ .<sup>8</sup>

<sup>8</sup> The constant phase  $\theta_0$  is of no importance in the microwave techniques. Therefore, we may disregard it.

In order to obtain the transfer function of the circuit under test, we take the above procedures in the two cases with and without the circuit under test inserted in Fig. 1. If the frequency spectra are  $\Omega_1(f)$  and  $\Omega_0(f)$  for the cases with and without the circuit respectively, then the transfer function  $\Omega_c(f)$  of the circuit under test is

$$\Omega_c(f) = \Omega_1(f)/\Omega_0(f). \quad (16)$$

This result means formally that the transfer function of the circuit under test can be determined completely by means of the test circuit of Fig. 1, if the frequency spectrum of the test pulse  $\Omega_0(f)$  does not vanish in the frequency region where the transfer function  $\Omega_1(f)$  exists.

But these procedures are considered to be less practical because the mathematical operations of Fourier transform are always necessary. It will be more practical to employ only the operations in the time domain.

For this purpose it will be convenient to impose some constraints on the test pulse and even on the circuit under test in some cases. We will give some explanations of functions of time and frequency on which the constraints are imposed.

The time-domain representation (waveform)

$$g(t)e^{j[\omega_0 t + \phi(t)]} \quad (17)$$

and the frequency-domain representation (frequency spectrum or transfer function)

$$R(f)e^{j\Theta(f)} \quad (18)$$

are combined with each other by the following Fourier transform pair:

$$R(f + f_0)e^{j\Theta(f+f_0)} = \int_{-\infty}^{\infty} g(t)e^{j\phi(t)}e^{-j2\pi f t} dt \quad (19)$$

$$g(t)e^{j\phi(t)} = \int_{-\infty}^{\infty} R(f + f_0)e^{j\Theta(f+f_0)}e^{j2\pi f t} df, \quad (20)$$

where  $g(t)$ ,  $\phi(t)$ ,  $R(f)$  and  $\Theta(f)$  are real functions of time  $t$  or frequency  $f$ , and

$$f_0 = \omega_0/2\pi. \quad (21)$$

Moreover, we will define the carrier frequency modulation  $F(t)$  and the delay time  $\tau(f)$  as

$$F(t) = \frac{1}{2\pi} \frac{d\phi(t)}{dt} \quad (22)$$

$$\tau(f) = -\frac{1}{2\pi} \frac{d\Theta(f)}{df}. \quad (23)$$

The constraints to be considered here are illustrated in Table II. Arrows in that table indicate the necessary

TABLE II  
CONSTRAINTS ON OBSERVED WAVEFORMS, TIME-DOMAIN REPRESENTATIONS AND FREQUENCY-DOMAIN REPRESENTATIONS

Observed Waveform (Synchronous Detection)	Time Domain	Frequency Domain	Band-Pass Low-Pass Analogy
a) no quadrature component, $Q(t)=0$	no carrier frequency modulation, $F(t)=0$	symmetrical or antisymmetrical amplitude, symmetrical delay time, $R(f+f_0) = \pm R(-f+f_0)$ , $\tau(f+f_0) = \tau(-f+f_0)$	valid
b) symmetrical or antisymmetrical in-phase component, no quadrature component, $I(t+t_0) = \pm I(-t+t_0)$ , $Q(t)=0$	symmetrical or antisymmetrical envelope, no carrier frequency modulation, $g(t+t_0) = \pm g(-t+t_0)$ , $F(t)=0$	symmetrical or antisymmetrical amplitude, flat delay time, $R(f+f_0) = \pm R(-f+f_0)$ , $d\tau(f)/df=0$	valid
c) symmetrical or antisymmetrical in-phase component, antisymmetrical or symmetrical quadrature component, $I(t+t_0) = \pm I(-t+t_0)$ , $Q(t+t_0) = \mp I(-t+t_0)$	symmetrical or antisymmetrical envelope, symmetrical carrier frequency modulation, $g(t+t_0) = \pm g(-t+t_0)$ , $F(t+t_0) = F(-t+t_0)$	flat delay time $d\tau(f)/df=0$	not always valid

and sufficient conditions. The proof of Table II is not described here because it can be obtained from (3), (6), (19), (20), (22) and (23) easily.

Case a) indicates the most important class of waveform or transfer function in the RF region. It is represented as an RF pulse without the carrier frequency modulation in the time domain and as a transfer function with symmetrical or antisymmetrical amplitude and symmetrical delay time in the frequency domain.<sup>9</sup>

Case c) indicates a class characterized by the flat delay time in the frequency domain. It is represented as an RF pulse having a symmetrical or antisymmetrical envelope and symmetrical carrier frequency modulation.

Case b) is the special case of a) and c). Its frequency-domain representation has symmetrical or antisymmetrical amplitude and flat delay time. And the time-domain representation has a symmetrical or antisymmetrical envelope and vanishing carrier frequency modulation.

It is well known that an RF pulse or a transfer function belonging to case a), or b) in the special case, is completely equivalent to the baseband pulse or baseband transfer function (band-pass low-pass analogy).<sup>10,11</sup> Therefore, we may apply the concepts in the baseband pulse techniques such as rise time, overshoot, etc., to the group of such pulses and such transfer functions.

It should be noticed that the conditions in Table II can be recognized easily by synchronous detection as illustrated in the first column. For example, a waveform

<sup>9</sup> The symmetrical and the antisymmetrical cases correspond to the band-pass and the band-elimination filters, respectively.

<sup>10</sup> V. D. Landon, "The band-pass low-pass analogy," Proc. IRE, vol. 24, pp. 1582-1584; December, 1936.

<sup>11</sup> P. R. Aigrain, B. R. Teare, Jr. and E. M. Williams, "Generalized theory of the band-pass low-pass analogy," Proc. IRE, vol. 37, pp. 1152-1155; October, 1949.

of a) is observed as one without the quadrature component where the waveform without quadrature component means the vanishing oscilloscope presentation for a certain local wave phase in the circuit of Fig. 1.

This fact affords the means to adjust a microwave linear circuit to satisfy the conditions of a), b) or c) in Table II. For example, the procedures of adjustment to obtain a filter with symmetrical or antisymmetrical amplitude and symmetrical delay time are as follows:

- 1) First, remove the filter from the circuit of Fig. 1 and ascertain that the test pulse has no carrier frequency modulation. (In the actual procedures ascertain that the observed waveform on the oscilloscope representation vanishes for a certain phase angle of local wave.)
- 2) Next, insert the filter into the circuit of Fig. 1 and adjust it to make its output have no carrier frequency modulation. (In the actual procedures adjust the filter to make the observed waveform on the oscilloscope representation vanish for a certain phase angle of local wave.)

By the above procedures the frequency spectra  $\Omega_0(f)$  and  $\Omega_1(f)$  in (16) are adjusted to have symmetrical or antisymmetrical amplitude and symmetrical delay time. Therefore, the transfer function  $\Omega_e(f)$  is made to have symmetrical or antisymmetrical amplitude and symmetrical delay time.

We will call the waveform observed when the filter is removed the test pulse. When the test pulse in the above procedure has carrier frequency modulation, we should remove it by conventional equalizing circuits.<sup>12</sup>

<sup>12</sup> A waveform equalizer employing the echo principle is used effectively in practice.

For this test pulse and these filters (linear circuits in the general case), adjusted by the above procedures, the band-pass low-pass analogy holds completely. Therefore, we can apply the parameters and concepts 4a)–4g) in the preceding section (Description of Measurement Principles) to this test pulse and these circuits.

The adjustment procedures in cases b) and c) in Table II can be understood similarly. Case b) is especially important because of its ideal transmission characteristics without phase distortions.

It is preferable to use the microwave step pulse (rectangular pulse) or the microwave short pulse as the test pulse in all cases for the same reasons as in the case of the baseband pulse techniques.

### EXPERIMENTS

When the microwave step pulse is used, the step response of a circuit is measured. In our experiments the over-all rise and fall times of the system are as small as 0.5 nsec. Waveform distortions such as overshoot, undershoot and echoes of the test pulse are negligibly small. Therefore, any microwave devices having a rise time larger than 1 nsec can be tested by means of the pulse generation and observation system described here.

When the microwave short pulse is used as the test pulse, the impulse response of a circuit is measured. The half amplitude duration of short pulse obtained in our experiments is 0.5 nsec (at 24-Gc) or 0.7 nsec (at 11-Gc). Therefore, delay resolution smaller than 1 nsec is obtained when a microwave transmission line is tested on the radar principle.

We can use the pulse generation and observation system described here for observing or measuring the pulse response of microwave nanosecond devices such as

- 1) pulse generator or modulator,<sup>4,13,14</sup>
- 2) detector,<sup>15</sup>
- 3) waveguide components,
- 4) delay equalizer and waveform equalizer,
- 5) traveling-wave amplifier,
- 6) waveguide transmission lines,
- 7) nonlinear elements (limiter, pulse regenerator, etc.).

The test results of pulse modulator (pulse generator), detector and waveguide filters are described briefly in the present paper. The frequency region treated here is that centered on 11 Gc. Detail of the system developed in the 24-Gc region is published elsewhere.<sup>16</sup>

<sup>13</sup> K. Miyauchi and O. Ueda, "High speed microwave switches using silver bonded diodes in 11-Gc region," to be published.

<sup>14</sup> K. Miyauchi and O. Ueda, "Nanosecond Pulse Generation in 11-Gc Region," *Proc. Professional Group on Microwave Transmission, Inst. Elec. Commun. Engrs. of Japan, Tokyo, Japan*; August, 1962.

<sup>15</sup> K. Miyauchi and O. Ueda, "Nanosecond Pulse Detectors in 11-Gc Region," *Elec. Commun. Lab., Tokyo, Japan, Internal Rept. No. 1899*; 1963.

<sup>16</sup> K. Miyauchi, "Generation and Observation of Nanosecond Carrier Pulses in 24-Gc Region," *Elec. Commun. Lab. Tech. J.*, vol. 11, pp. 1557–1614; September, 1962.

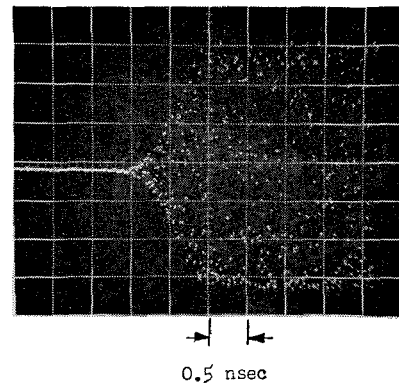


Fig. 3—Envelope waveform of 11-Gc step pulse observed by heterodyne detection.

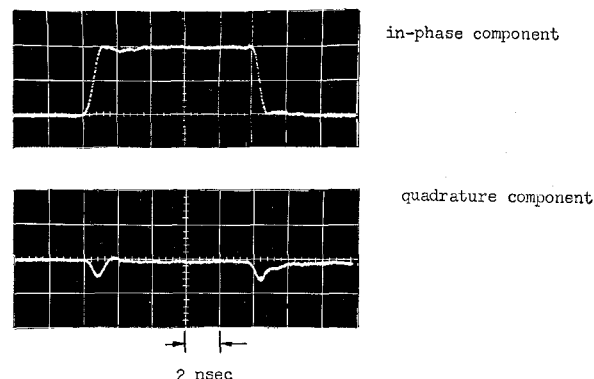


Fig. 4—Amplitude waveforms of 11-Gc rectangular pulse observed by synchronous detection.

The pulse modulators used here are microwave switches employing semiconductor diodes GSB1, GSB2 SiSBR, SiSBY, 1N263, 1N78 or 1N31. The silver-bonded diodes GSB1, GSB2, SiSBR and SiSBY<sup>17,18</sup> are the most satisfactory for these applications. Modulation with a baseband step pulse was used to examine the applicability of diodes. The synchronous detector and the sampling oscilloscope were used to observe the pulse waveforms. Detail of the experiments is described in another paper.<sup>13</sup> When the best detector is used, the observed amplitude rise and fall times (10–90 per cent) of the 11-Gc step pulse are 0.5–0.76 nsec, when overshoot or undershoot are negligibly small; 0.4 nsec, when overshoot or undershoot of about 20 per cent is allowed. The rise time of the sampling oscilloscope (H.P. Model 187B) used here is presumably 0.35 nsec.

Fig. 3 is the envelope of the 11-Gc step pulse observed by heterodyne detection. Fig. 4 illustrates the in-phase and quadrature components of the 11-Gc rectangular pulse generated by the pulse modulator using the silver-bonded diode SiSBR.

<sup>17</sup> S. Kita, T. Okajima and M. Chung, "Parametric amplifier using a silver-bonded diode," *IRE TRANS. ON ELECTRONIC DEVICES*, vol. ED-8, pp. 105–109; March, 1961.

<sup>18</sup> S. Kita, "Microwave applications of the silver-bonded diode," *Electronics*, vol. 35, pp. 86–87; May, 1962.

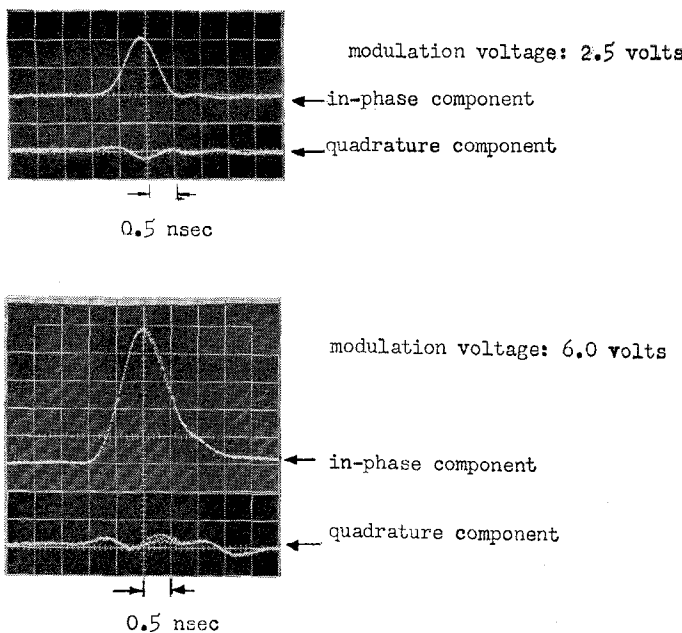


Fig. 5—Amplitude waveforms of 11-Gc short pulses generated by waveguide switch using a silver-bonded diode GSB2.

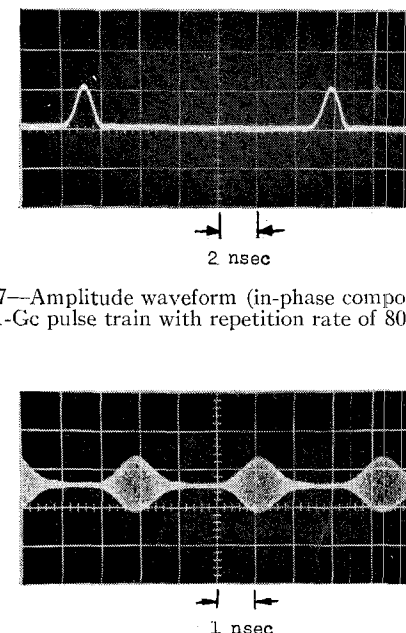


Fig. 7—Amplitude waveform (in-phase component) of 11-Gc pulse train with repetition rate of 80 Mc.

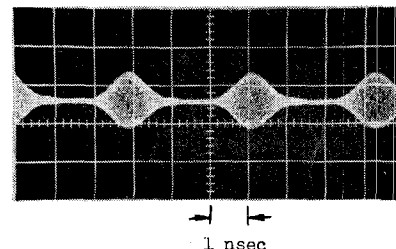


Fig. 8—Envelope waveform of 11-Gc pulses train with repetition rate of 320 Mc.

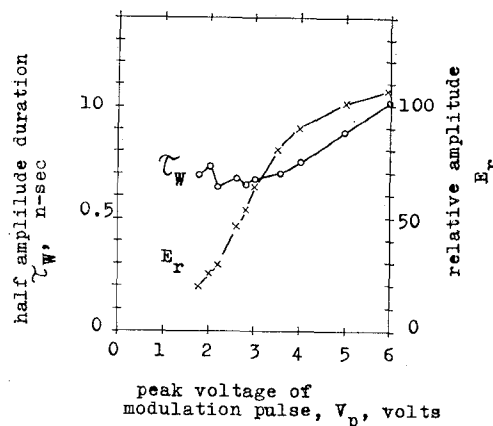


Fig. 6—Characteristics of 11-Gc short pulse generated by a waveguide switch using GSB2. Waveguide switch: transmission type, microwave input power: 5 milliwatts, dc bias voltage: -5 volts.

Modulation with a baseband short pulse was also examined. Fig. 5 illustrates the observed amplitude waveforms of 11-Gc short pulses. The half amplitude duration of the applied baseband short pulse is about 0.6 nsec. Fig. 6 shows the observed half amplitude duration and relative amplitude of the 11-Gc short pulse as a function of incident modulation voltage when a silver-bonded diode GSB2 is used as the modulator. When the modulation voltage is comparatively large, the waveform of 11-Gc pulses becomes asymmetrical. This phenomenon is considered to be due to the hole storage effect.<sup>13</sup> As a result of these experiments a microwave short pulse with half amplitude duration of about 0.7 nsec was obtained.

Microwave pulse trains with high repetition rates were also generated and their amplitude waveforms were

observed. Fig. 7 illustrates an 11-Gc pulse train with a repetition rate of 80 Mc. This pulse train is generated with the SiSBR diode switch modulated by a 80-Mc baseband pulse train.

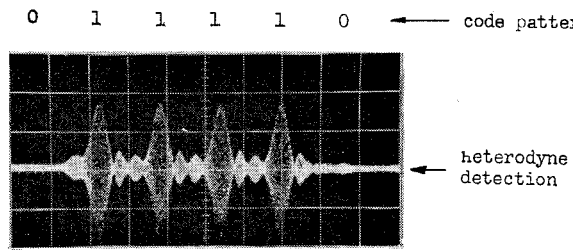
At a higher repetition rate, baseband pulse trains are not available. Therefore VHF sinusoidal waves are used as the modulation signals. Fig. 8 illustrates an 11-Gc pulse train with repetition rate of 320 Mc generated by the sinusoidal modulation. These modulators may be used as the timing portion in a high-speed PCM repeater.

Fig. 9 illustrates an example of code pulse train with a bit rate of 160 Mc. The waveforms (a) and (b) were obtained by heterodyne and quadratic detection, respectively. It is observed that heterodyne detection is particularly useful for the observation of weak echoes.

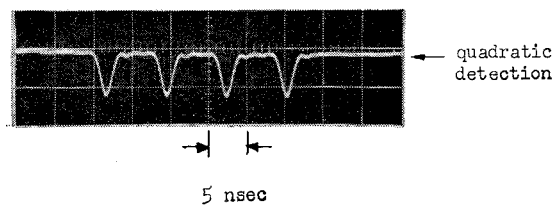
Several detectors employing 1N31, 1N78 and 1N358 diodes were tested by the pulse generation and observation system developed here. Fig. 10 illustrates an example of the diode mount designed for the tripolar diode 1N358. A short high-impedance section is attached in a part of the output coaxial line to improve the pulse response, because the diode has a comparatively large output capacitance.

These detectors were employed as the synchronous detectors in Fig. 1. The output pulse was observed for the incident rectangular pulse. The amplitude rise times (10-90 per cent) of observed pulses were from about 0.5 to 1.4 nsec typically for the incident 11-Gc pulse without overshoot. A typical example is shown in Fig. 11.

The rise time of the observed step pulse waveform represents the over-all rise time of the pulse generation



(a)



(b)

Fig. 9—Example of code pulse train. Bit rate is 160 Mc. Waveforms observed by heterodyne and quadratic detection are illustrated.

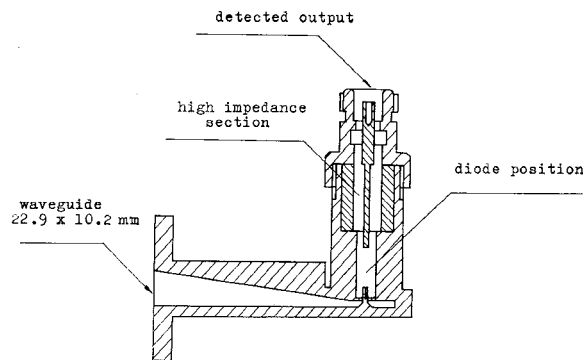


Fig. 10—Diode mount  $D_6$  for detection of 11-Gc nanosecond pulses.

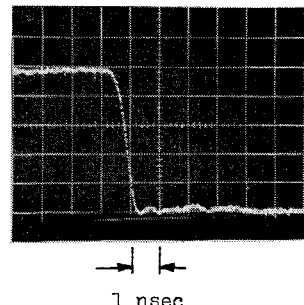
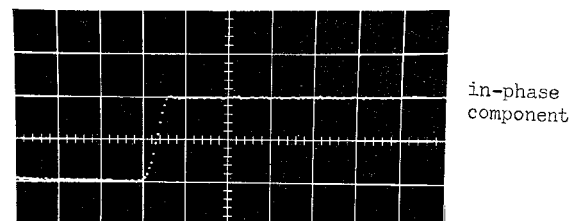


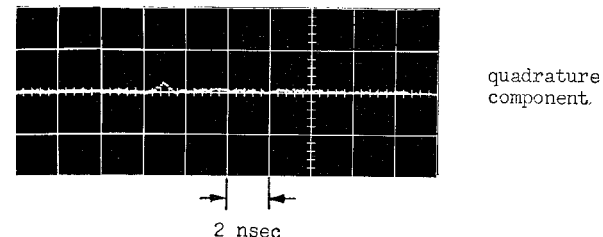
Fig. 11—Step response of nanosecond pulse detector  $D_2$ . In-phase component is illustrated.

and observation system which is composed of the microwave pulse generator, the waveguides, the isolators, the pulse detector and the sampling oscilloscope. All of these devices operate linearly. Therefore, this system can be used to measure the pulse response of an 11-Gc pulse device having a rise time larger than 1 nsec, *i.e.*, twice that of the system rise time of 0.5 nsec, when the best detector is employed.

We will show some examples of adjusting and measuring the microwave filters. Fig. 12 is a microwave step pulse used for the test of filters. The duration of quadrature component is much smaller than the rise time of

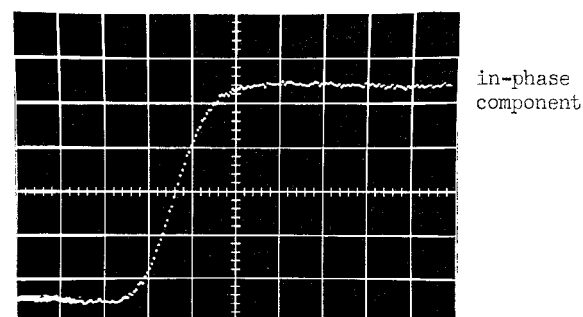


in-phase component

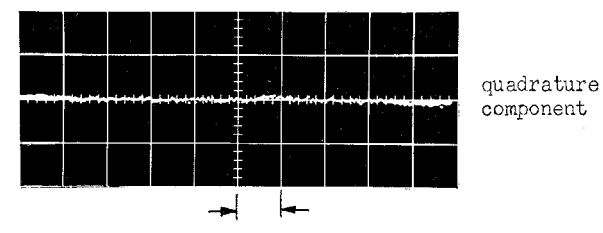


quadrature component

Fig. 12—11-Gc step pulse used for test of filters.



in-phase component



quadrature component

Fig. 13—Step response of waveguide Thomson filter with four cavities. Bandwidth: 235 Mc; center frequency: 11-Gc.

the tested filters. Therefore, it has little contribution to the measurement, and the equalization procedure is not necessary.

Fig. 13 illustrates the observed response of a Thomson filter with four cavities adjusted by the pulse generation and observation system. The adjustment of the center frequency of each cavity is performed by making the quadrature component of the output pulse of the composite filter vanish. The practical procedure is simple and easy. It requires one to adjust only the stubs of cavities and the phase shifter of the local wave repeatedly, and to make the observed waveform vanish at a certain local phase.

Fig. 14 illustrates the step responses of a single tune filter and a maximally flat filter with three cavities. The maximally flat filter has been adjusted by the usual method using a sweep oscillator.

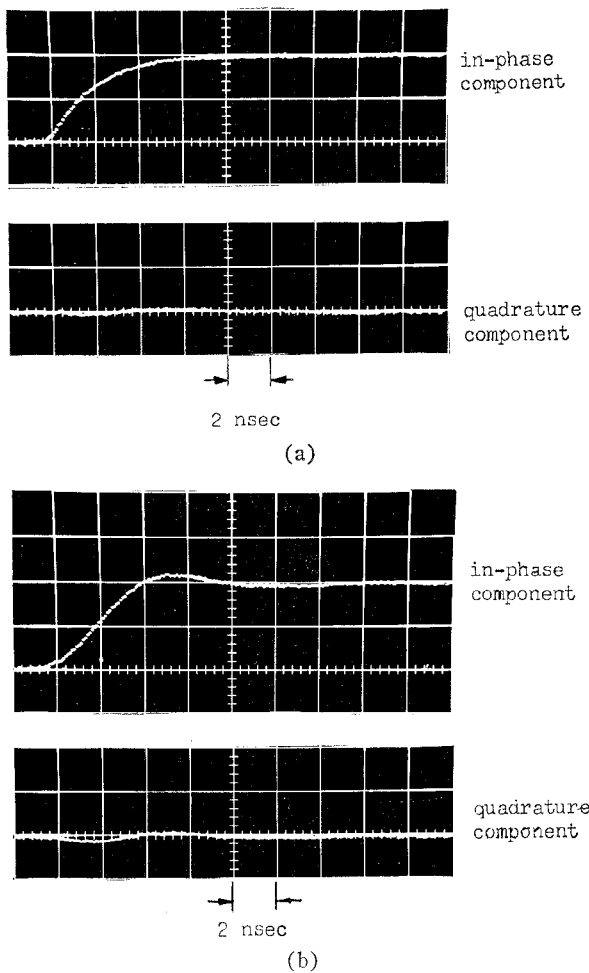


Fig. 14—Step response of waveguide filters. (a) Single tune filter. Bandwidth: 157 Mc; center frequency: 11-Gc. (b) Maximally flat filter (three cavities). Bandwidth: 233 Mc; center frequency: 11-Gc.

### CONCLUSIONS

The ordinary method of waveform observation employing a quadratic detector has many disadvantages. The quadratic detector prevents the waveform observation system from being analyzed by linear mathematics. Moreover, its sensitivity is too poor to be used together with the sampling oscilloscope, when microwave nanosecond pulses are to be observed.

These disadvantages can almost be removed when we use a synchronous or a heterodyne detector instead of the quadratic detector. It was concluded theoretically and experimentally that the synchronous detector gives the most precise information of the pulse waveforms. Employing it, the analysis of microwave pulse devices becomes possible on the same standpoints as in the baseband pulse techniques. The parameters such as rise and fall times and half amplitude duration of a pulse have their real importance in the RF region when the synchronous detector is employed.

The test and adjustment of microwave devices employing the synchronous detector was also described. Although the description was concerned only with the system using the sampling oscilloscope, it accommodates also to the ordinary conventional oscilloscope.

Therefore, the procedure described here is expected to be a rapid and simple method to test and adjust the microwave devices in place of the ordinary method in the frequency domain.

### APPENDIX I

#### WAVEFORM OBSERVATION EMPLOYING A HETERODYNE DETECTOR

Let us assume that a signal pulse train

$$G(t) = \sum_{-\infty}^{\infty} G_m(t),$$

$$G_m(t) = g(t - mT) \cos [\omega_0 t + \phi(t - mT)] \quad (24)$$

is mixed with a local wave

$$E(t) = E_L \cos \omega_1 t \quad (25)$$

in the heterodyne detector. The detector output becomes

$$S_m(t) = H(E_L)g(t - mT) \cos [\Delta\omega t - \phi(t - mT)], \quad (26)$$

where  $H(E_L)$  is a function of  $E_L$  determined by the nonlinearity of the detector, and

$$\Delta\omega = \omega_1 - \omega_0. \quad (27)$$

We will assume that the signal  $S_{nM}(t)$  is sampled at the instants  $n(MT + \Delta T)$  by a sampling oscilloscope, where  $M$  is an integer. The sampled value is

$$U(n\Delta T)$$

$$= H(E_L)g(n\Delta T) \cos [n\Delta\omega MT + n\Delta\omega\Delta T - \phi(n\Delta T)] \quad (28)$$

for every integer  $n$ .

When  $\Delta T$  is so small that  $n\Delta T$  may be regarded as a continuous variable  $x$ , we obtain

$$U(x) = H(E_L)g(x) \cos [\omega_i x + \phi(x)]. \quad (29)$$

Eq. (29) is an RF pulse waveform whose envelopes and instantaneous phase modulation are identical with those of the original pulse train (24). The angular carrier frequency  $\omega_i$  is given as

$$\omega_i =$$

$$-\frac{(MT + \Delta T)\Delta\omega}{\Delta T} - \frac{2\pi}{\Delta T} \left[ \left[ -\frac{(MT + \Delta T)\Delta\omega}{2\pi} \right] \right], \quad (30)$$

where the symbol  $\left[ \left[ \alpha \right] \right]$  denotes the largest integer which does not exceed  $\alpha$ .

### APPENDIX II

#### MEASUREMENT SYSTEMS EMPLOYING NONIDEAL DEVICES

Here we will treat the measurement systems employing a nonideal oscilloscope and a nonideal synchronous detector.

It is assumed that a nonideal oscilloscope is represented as a baseband filter connected to an ideal ob-

servation device with an infinitesimally small rise time. For the conventional oscilloscope this assumption is self-evident. For the sampling oscilloscope it can be derived from a convolution integral which describes the sampling operation.

The nonideal synchronous detector is assumed to be represented as a cascade circuit composed of three devices, *i.e.*, an RF filter, an ideal synchronous detector and a baseband filter.

The operation of the ideal synchronous detector is to convert an input frequency spectral component with frequency  $f$  and phase  $\psi$  into an output frequency spectral component with frequency  $f-f_0$  and phase  $\psi-\theta$  linearly and independently. This fact, which is derived from the property of the synchronous detector as a frequency converter, is important in the following discussions.

#### Waveform Measurement

Two equivalent circuits of the measurement system are illustrated in Fig. 15(a). The circuit *A* is one obtained directly from the original circuit as illustrated in Fig. 1.  $F_R$  is an RF filter representing the RF characteristics of the synchronous detector.  $D$  is an ideal synchronous detector.  $F_B$  and  $F_S$  are baseband filters representing the baseband characteristics of the synchronous detector and the sampling oscilloscope respectively. Let the transfer function of the filter  $F_R$  be  $\Omega_1(f)$ , and that of the filters  $F_B$  and  $F_S$  be connected in cascade be  $\Omega_2(f)$ .

Here the author will propose that the precise measurement of waveform can be made if the RF filter  $F_R$  fulfills the condition of case a) in Table II. The wide-band detector may be considered to fulfill this condition best of all. In this case the circuit *A* in Fig. 15(a) can be rewritten as the circuit *B*. The reason is that an input signal with a frequency spectrum  $\Omega(f)$  is converted to an output signal with a frequency spectrum

$$K\Omega(f+f_0)\Omega_1(f+f_0)\Omega_2(f)e^{-j\theta}$$

in the circuit *B* as well as in the circuit *A*, where  $K$  is a constant.

The circuit *B* is considered as a measurement system employing an ideal synchronous detector and an oscilloscope whose rise time is determined with a transfer function  $\Omega_2'(f) = \Omega_1(f+f_0)\Omega_2(f)$ . Therefore, the in-phase and quadrature components of a pulse waveform can be measured independently under the common influence of the rise time of a baseband transfer function  $\Omega_2'(f)$ .

This situation allowed us to analyze the in-phase and quadrature components as baseband pulses separately. Therefore the concepts in the baseband techniques can be applied completely to this measurement system.

#### Test and Adjustment of Linear Circuit

Some equivalent circuits of Fig. 1 are illustrated in Fig. 15(b). The symbols  $F_R$ ,  $D$ ,  $F_B$  and  $F_S$  are identical with those in Fig. 15(a).  $P$  and  $C$  are the test pulse generator and the linear circuit to be tested, respectively.

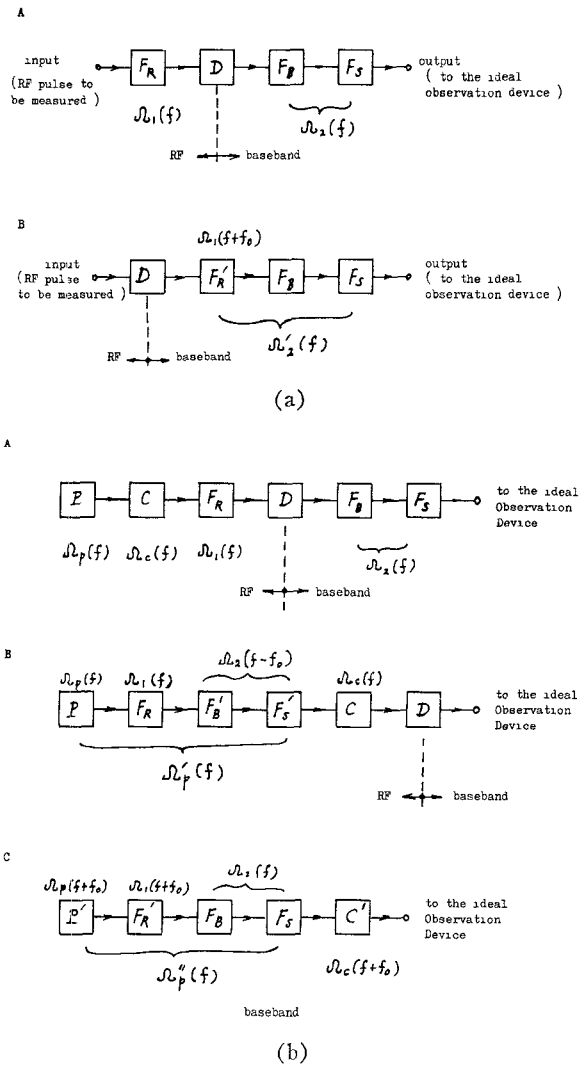


Fig. 15—(a) Equivalent circuits of waveform measurement system. (b) Equivalent circuits of system for test and adjustment of linear circuit.

Circuit *A* is derived directly from the original circuit in Fig. 1. Circuit *B* is obtained by rewriting *A*. In circuit *B*, the baseband filters  $F_B$  and  $F_S$  are removed, and RF filters  $F_B'$  and  $F_S'$  whose over-all transfer function is  $\Omega_2(f-f_0)$  are inserted into the RF part.

It is apparent that circuits *A* and *B* have the identical output

$$K\Omega_p(f+f_0)\Omega_c(f+f_0)\Omega_1(f+f_0)\Omega_2(f)e^{-j\theta},$$

where  $\Omega_p(f)$  and  $\Omega_c(f)$  are the output spectrum of the test pulse generator and the transfer function of the circuit under test, respectively.

Circuit *B* is considered as a measurement system employing an ideal synchronous detector and a test pulse generator whose output spectrum is  $\Omega_p'(f) = \Omega_p(f)\Omega_1(f)\Omega_2(f-f_0)$ .

When  $\Omega_p'(f)$  and  $\Omega_c(f)$  are adjusted to fulfill the condition illustrated in case a) of Table II, the circuit *A* or *B* can be also reduced to a baseband circuit as illustrated in *C*.